research article

Co-treatment with vactosertib, a novel, orally bioavailable activin receptor-like kinase 5 inhibitor, suppresses radiotherapy-induced epithelial-to-mesenchymal transition, cancer cell stemness, and lung metastasis of breast cancer

Jiwon Choi[1,2], Jiyoung Park[1,2], Ilyoung Cho[1], Yhunyhong Sheen[1]

[1] College of Pharmacy, Ewha Womans University, Seoul, Republic of Korea
[2] National Center for Efficacy Evaluation for Respiratory Disease Products, Korea Institute of Toxicology, Republic of Korea

Correspondence to: Yhunyhong Sheen, 52, Ewhayeodae-gil, Seodaemun-gu, Seoul, Republic of Korea, 03760. E-mail: yysheen@ewha.ac.kr

Disclosure: No potential conflicts of interest were disclosed.

Background. Acquired metastasis and invasion of cancer cells during radiotherapy are in part due to induction of epithelial-to-mesenchymal transition (EMT) and cancer stem cell (CSC) properties, which are mediated by TGF-β signaling. Here we evaluated the anti-metastatic therapeutic potential of vactosertib, an orally bioavailable TGF-β type I receptor (activin receptor-like kinase 5, ALK5) inhibitor, via suppression of radiation-induced EMT and CSC properties, oxidative stress generation, and breast to lung metastasis in a breast cancer mouse model and breast cancer cell lines.

Materials and methods. Co-treatment of vactosertib with radiation was investigated in the 4T1-Luc allografted BALB/c syngeneic mouse model and in 4T1-Luc and MDA-MB-231 cells. The anti-metastatic therapeutic potential of vactosertib in breast cancer was investigated using fluorescence immunohistochemistry, real-time quantitative reverse transcription-polymerase chain reaction, western blotting, wound healing assay, mammosphere formation assay, and lung metastasis analysis *in vitro* and *in vivo*.

Results. Radiation induced TGF-β signaling, EMT markers (Vimentin, Fibronectin, Snail, Slug, Twist, and N-cadherin), CSC properties (expression of pluripotent stem cell regulators, mammosphere forming ability), reactive oxygen species markers (NOX4, 4-HNE), and motility of breast cancer cells *in vitro* and *in vivo*. Vactosertib attenuated the radiation-induced EMT and CSC properties by inhibiting ROS stress in breast cancer. Moreover, vactosertib combined with radiation showed a significant anti-metastatic effect with suppression of breast to lung metastasis *in vivo*.

Conclusions. These results indicate that inhibition of TGF-β signaling with vactosertib in breast cancer patients undergoing radiotherapy would be an attractive strategy for the prevention of cancer metastasis and recurrence.

Key words: vactosertib; transforming growth factor-β (TGF-β); radiotherapy; epithelial-to-mesenchymal transition; cancer stem cell; breast cancer

Introduction

Radiotherapy is an essential treatment modality for multiple malignancies. Currently, over 60% of all cancer patients receive radiotherapy, either alone or in combination with other therapy such as surgery or chemotherapy.[1,2] Despite advances in radiotherapy, cancer cells that survive after ra-

diotherapy acquire treatment resistance.[3,4] Radio-resistance of cancer cells reduces the effectiveness of radiotherapy and limits the delivery of a sufficient amount of radiation to the tumor, leading to normal tissue damage and fibrosis along with an increase in radiation dose.[4] In addition, metastasis is a serious hurdle for successful cancer treatment and a leading cause of cancer death in patients with breast cancer. However, no therapeutic strategy is yet available to reduce metastasis.[5,6] Therefore, it is important to understand the mechanism of cancer metastasis after radiotherapy with the aim of developing an effective therapeutic strategy.

Based on the emerging understanding of the molecular mechanism of radio-resistance of cancer, transforming growth factor-β (TGF-β) has emerged as a key component that functions in the metastatic relapse after radiotherapy.[4,7] TGF-β controls numerous functions in cancer such as cell proliferation, angiogenesis, epithelial-to-mesenchymal transition (EMT), stemness of cancer cells, metastasis, and immune responses. Therefore, regulation of TGF-β signaling will play a key role in controlling cancer progression and metastasis.[4,8] Acquired metastatic potential during radiotherapy is in part due to TGF-β-induced EMT and stemness of cancer cells.[4,9,10] EMT is associated with various biological processes including embryogenesis, wound healing, fibrogenesis, and cancer metastasis.[6,9] During EMT in the tumor microenvironment, epithelial cells lose their polarized organization and go through genetic changes to become mesenchymal stem cells with migratory and invasive capabilities, and cancer stem cells (CSCs) are developed.[4,9,11] CSC properties, such as self-renewal activity, the ability to differentiate into different types of cancer cells, and resistance to anti-cancer therapies, provide an explanation for metastasis to distant organs and cancer recurrence.[9,12] In the *in vitro* assays, TGF-β-treated breast cancer cells grow as nonadherent spheroids (mammospheres), a characteristic associated with stem cells.[13] These effects are activated by the canonical (Smad-dependent) TGF-β pathway that includes TGF-β type I receptor (activin receptor-like kinase 5, ALK5) phosphorylation of Smad2/3 (p-Smad2/3).[14] These findings have led to the development of highly specific TGF-β/ALK5 inhibitors that block the binding of TGF-β to its receptor.

Vactosertib (EW-7197) is a highly potent, selective, and orally bioavailable TGF-β signaling inhibitor that also targets ALK5.[15,16] Studies in various animal models, showed that vactosertib is rapidly absorbed following oral administration with demon-

strated its safety and efficacy.[9,17-19] Vactosertib treatment weakened TGF-β/Smad signaling and cancer cell migration, invasion, and metastasis *in vitro* and *in vivo* models of breast cancer, melanoma, pancreatic cancer, and prostate cancer.[18,20,21] Furthermore, vactosertib inhibited paclitaxel-induced EMT and CSC characteristics, and attenuated lung metastasis after paclitaxel treatment in a breast cancer mouse model.[9] Therefore, considering the critical role of vactosertib in inhibition of metastasis, vactosertib combination with chemotherapy and/or radiotherapy could be a candidate strategy for breast cancer therapy considering its critical role in inhibition of metastasis. Based on the favorable pharmacologic, pharmacokinetic, and toxicologic profiles of vactosertib, a first-in-human phase I study of vactosertib was conducted in patients with advanced stage solid tumors.[16,22] Clinical studies of vactosertib in combination with other chemotherapies are ongoing in patients with various cancer types like gastric cancer (NCT03698825), non-small cell lung cancer (NCT03732274), colorectal or gastric cancer (NCT03724851), desmoid tumor (NCT03802084), and multiple myeloma (NCT03143985).

Based on the non-clinical and clinical studies of vactosertib, we hypothesized that vactosertib might repress cancer metastasis after radiotherapy by inhibiting TGF-β/Smad-induced EMT and stemness of cancer cells. In this study, we take the first steps towards exploring whether vactosertib shows therapeutic benefits to breast cancer patients undergoing radiotherapy by investigating the effects of combined therapy of vactosertib with radiotherapy in *in vitro* and *in vivo* models of breast cancer. We demonstrated that blocking radiotherapy-induced TGF-β signaling with the ALK5 inhibitor vactosertib can inhibit development of EMT and cancer cell stemness, reactive oxygen species (ROS) stress generation, and lung metastasis of breast cancer.

Materials and methods

Chemicals

N-[[4-([1,2,4]Triazolo[1,5-a]pyridin-6-yl)-5-(6-methylpyridin-2-yl)-1*H*-imidazol-2-yl]methyl]-2-fluoroaniline (vactosertib) was synthesized by Dr. D. K. Kim (Ewha Womans University, Seoul, Korea).

Gene analysis of open-source clinical data

Gene-expression raw data of breast cancer patients from the Kreike dataset were downloaded from

'R2: Genomics Analysis and Visualization Platform (https://r2.amc.nl)'.[23] Gene Set Enrichment Analysis (GSEA) was performed to evaluate correlation between radiation response gene sets and recurrence of breast cancer.

Cell culture and cell irradiation

The 4T1-Luc mouse breast cancer cells and MDA-MB-231 human breast cancer cells were obtained from the American Type Culture Collection. The 4T1-Luc cells were grown in Dulbecco's Modified Eagle's medium (DMEM) (GenDEPOT, Katy, TX, USA) containing hydroxyethyl piperazineethanesulfonic acid (HEPES) sodium salt (Sigma-Aldrich, St. Louis, MO, USA), sodium bicarbonate (Sigma-Aldrich, St. Louis, MO, USA), 5% fetal bovine serum (FBS) (GenDEPOT, Katy, TX, USA), and 100X penicillin-streptomycin solution (GenDEPOT, Katy, TX, USA). MDA-MB-231 cells were grown in Roswell Park Memorial Institute (RPMI) 1640 culture medium (Gibco, Grand Island, NY, USA) containing HEPES sodium salt, sodium bicarbonate, sodium pyruvate solution (Gibco, Grand Island, NY, USA), 5% FBS, and 100X penicillin-streptomycin solution. Cells were grown at 37°C in 5% CO_2. Cells were seeded in culture plates and maintained with serum-reduced (0.2% FBS) medium for 16 h for starvation. Cells were pretreated with vactosertib (100 nM) for 30 min and then irradiated with 10 Gy. After 24 h of incubation, *in vitro* assays were conducted.

Experimental mouse breast cancer model for co-treatment with vactosertib and radiation

All experimental procedures were approved by the Animal Care Committee of Ewha Womans University and complied with the NIH Guide for the Care and Use of Laboratory Animals (Institute of Laboratory Animal Resources, National Research Council, WA, USA). Female BALB/c mice were purchased from Central Lab Animal Inc. (Korea). Four to five mice were housed per cage at 21°C with 50% humidity and a 12-h light cycle. A total of 4 X 10⁴ 4T1-Luc cells were injected into the fourth mammary fat pad of female BALB/c mice. When the tumor volume reached 70-100 mm³, mice were randomly divided into three groups: control, radiation, and vactosertib + radiation group (n = 8/group). The control group received no treatment, the radiation group received whole body irradiation with 4 Gy/day for three days, and the vactosertib + radiation group was treated with vactosertib 2.5 mg/kg *p.o.* for two weeks and concurrently received whole body irradiation 4 Gy/day for three consecutive days.

India ink staining

Mice were sacrificed, and 15% India ink (Hardy Diagnostics) in PBS was injected into the lung through the bronchi using a 1 ml syringe. After washing the stained lungs, the number of metastatic nodules on the surface of the left lobe of the lung was counted.

Microarray analysis

Total RNA from breast cancer pieces (100 mm³) was isolated using Trizol solution (Invitrogen, Carlsbad, CA, USA) and purified using a RNeasy column (Qiagen, Chatsworth, CA, USA). Aliquots of the RNA samples from each group of mice were pooled (n=8). Experiments were performed on Affymetrix GeneChip Mouse Gene 2.0 ST arrays that cover 26,515 genes (RefSeq-Entrez gene count; Affymetrix, Santa Clara, CA, USA). Arrays were scanned using a GeneChip™ Scanner 3000 7G controlled by GeneChip® Operating Software (GCOS, Affymetrix). Scanned data were analyzed with GeneChip® Operating and Expression Console Software (Affymetrix) and GenPlex v3.0 (ISTECH, Goyang, Korea). The signal intensity of each gene from different arrays was normalized according to the total intensity of all genes in each array to compare the results of separate hybridization experiments. Normalized signals of each array were compared to determine the fold induction or reduction in the gene expression between samples.

Fluorescence immunohistochemistry (IHC) assay

For detecting p-SMAD2/3, SNAIL, VIMENTIN, FIBRONECTIN, NANOG, OCT4, SOX2, c-MYC and KLF4 by fluorescence immunohistochemistry assay, formalin-fixed and paraffin-embedded sections of mouse tissues were dewaxed in an OTTIX bath (Diapath, Martinengo, Italy) and blocked with solution containing 5% BSA (GenDEPOT, Katy, TX, USA) and 0.1% Triton 100X (Merk, Darmstadt, Germany). Slides were incubated with a primary antibody mixture of anti-p-SMAD2/3 mouse IgG (Santa Cruz Biotechnology, Santa Cruz, CA, USA), anti-SNAIL rabbit IgG (Cell Signaling, Beverly,

MA, USA) and anti-VIMENTIN mouse IgG (Santa Cruz Biotechnology, Santa Cruz, CA, USA); a mixture of anti-FIBRONECTIN mouse IgG (BD Biosciences, San Diego, CA, USA), anti-NANOG rabbit IgG (Abcam, Cambridge, MA, USA) and anti-OCT4 rabbit IgG (Abcam, Cambridge, MA, USA); or a mixture of anti-SOX2 rabbit IgG (Abcam, Cambridge, MA, USA), anti-c-MYC mouse IgG (Santa Cruz Biotechnology, Santa Cruz, CA, USA) and anti-KLF4 rabbit IgG (Abcam, Cambridge, MA, USA). A mixture of Alexa 488-conjugated anti-rabbit IgG (Cell Signaling, Beverly, MA, USA) F(ab') fragments were used for visualization of SNAIL, NANOG, OCT4, SOX2 and KLF4 proteins. A mixture of Alexa 488-conjugated anti-mouse IgG (Cell Signaling, Beverly, MA, USA) F(ab') fragments were used for visualization of p-SMAD2/3, VIMENTIN, FIBRONECTIN, and c-MYC proteins. Slides were counterstained with 4'6-diamidino-2-phenylindole (DAPI). Fluorescence was visualized using an Axio observer inverted microscope (Carl Zeiss, Jena, Germany).

Western blot analysis

Mouse tissues and cultured cells were homogenized in RIPA buffer [50 mM Tris-HCl (pH 7.4), 1% NP-40, 150 mM NaCl, 0.5% sodium deoxycholate, 0.1% sodium dodecyl sulfate, 1 mM EDTA, 1 mM Na_3VO_4, 50 mM NaF, 1 mM phenylmethylsulfonyl fluoride, and a protease inhibitor cocktail (Roche, Mannheim, Germany)] for 30 min on ice. Lysates were centrifuged at 13,000 rpm and 4°C for 10 min. The protein content of the lysates was determined by the BCA protein assay kit (Thermofisher Scientific, Waltham, MA, USA). Proteins (5 – 10 μg) were separated by 6–12% sodium dodecyl sulfate-polyacrylamide gel electrophoresis and then transferred to nitrocellulose (Whatman, Middlesex, UK) or polyvinylidene fluoride membranes (Millipore, Billerica, MA, USA). The membrane was blocked with 5% bovine serum albumin (BSA) (GenDEPOT, Katy, TX, USA) or 5% skim milk (BD Biosciences, San Diego, CA, USA) and incubated at room temperature for 1 h with specific primary antibodies, as listed in Supplementary Table A.1. Following washes in 1X Tris-buffered saline including 0.1% Tween®20 detergent, the membrane was incubated with horseradish peroxidase-conjugated secondary antibody for 30 min. Proteins were detected by an enhanced chemiluminescence kit (ATTO, Tokyo, Japan). Band intensities were analyzed using a LAS-3000 densitometer (Fujifilm, Tokyo, Japan).

Mammosphere-forming assay

Cells were seeded in 6 cm plates and incubated for 24 h for attachment. Cells were incubated with serum-reduced (0.2% FBS) medium for 16 h for starvation and irradiated with 10 Gy with or without 30-min pretreatment with 100 nM vactosertib. After 1, 2, 6, and 24 h of incubation, we harvested the adherent cells with trypsin-EDTA and reseeded the cells in ultra-low attachment dishes. Cells were incubated in DMEM/F-12 (1:1) (GenDEPOT, Katy, TX, USA) supplemented with B-27™ Supplement (50X) (Gibco Laboratories, Grand Island, NY, USA), 10 ng/ml bFGF (Invitrogen, Carlsbad, CA, USA), and 10 ng/ml EGF (Sigma-Aldrich, St. Louis, MO, USA). To measure mammosphere-forming efficiency (MSFE), the number of spheres (> 50 μm) was counted after one week. MSFE was determined as the number of spheres divided by the original number of cells seeded and is presented as %.

Wound healing assay

The 4T1-Luc cells were seeded in 6 cm culture plates and incubated for 24 h for attachment. Cells were incubated with serum-reduced (0.2% FBS) medium for 16 h for starvation and irradiated with 10 Gy with or without 30-min pretreatment with vactosertib (100 nM). After 24 h of incubation, 2.1 X 10^4 cells were seeded in each well of a cell culture insert (Ibidi, Munich, Germany) in a 35 mm plate. When cells reached 80% confluence, the insert was removed and 1 mL medium containing 0.2% FBS was added. After 20 h of incubation, the wound area was observed using an Axio observer inverted microscope (Carl Zeiss, Jena, Germany). The closure of the wound area was calculated as a percentage of the initial wound area.

DNA extraction from blood from the breast cancer mouse model

Blood from each group of mice was collected after 2 weeks treatment of vactosertib. The collected blood was centrifuged at 1,500 rpm and 4°C for 15 min and the supernatant was discarded. The cell pellet was resuspended in extraction solution (0.1 M ethylene-diamine-tetraacetic acid (EDTA), 0.2 M NaCl, 0.05 M Tris-HCl (pH 8.0), 0.5% SDS, 50 mg/mL RNase). Proteolytic enzyme K (100 mg/mL, EM Science, Gibbstown, NJ, USA) was mixed with the suspension and the suspension was incubated for 2–3 h at 55°C. Phenol/chloroform (1:1) was mixed with the suspension and the sample was centri-

fuged at 1,500 rpm at room temperature (RT) for 5 min. The supernatant was transferred into a new tube and chloroform/isoamyl alcohol (24:1) was added; the mixture was centrifuged at 1,500 rpm at RT for 5 min. The supernatant was transferred into a new tube and mixed with 3 M sodium acetate (pH 5.2) and ethanol; the mixture was shaken until the DNA precipitated. A glass pipette that had been formed into a loop over a Bunsen burner was used to capture the DNA. The DNA was washed in 70% ethanol and dried by vacuum. DNA was dissolved in ddH_2O to measure the purity and then analyzed by quantitative reverse transcription - polymerase chain reaction (qRT-PCR).

RNA extraction, RT-PCR, and qRT-PCR analyses

Total RNA was isolated from mouse tissues and cultured cells using Ambion's TRizol reagent. cD-NAs were synthesized from 1 µg of total RNA using M-MLV reverse transcriptase (BIONEER, Oakland, CA, USA) and random primers (Promega, Madison, WI, USA). Synthesized cDNAs were amplified for PCR using SYBR Green real-time quantitative RT-PCR reagent (Applied Biosystems, Foster City, CA, USA). The primers are listed in Supplementary Table A.2. To amplify cDNA a Step-One Real-time PCR system (Applied Biosystems, Foster City, CA, USA) was used.

Statistical analysis

Data are expressed as mean ± standard error of the mean (SEM). Data represent means of three independent experiments performed in triplicate. Statistical values were determined by one-way analysis of variance (ANOVA) with Bonferroni post-hoc test. Asterisks are used to indicate statistical significance (*, **, and *** indicate $p < 0.05$, $p < 0.01$, and $p < 0.005$, respectively).

Results

Breast cancer recurrence and metastasis after radiotherapy is related to the upregulation of the TGF-β signaling and vactosertib inhibits breast cancer metastasis to the lung.

We first performed an *in silico* analysis to examine the possible mechanism for radiotherapy-induced TGF-β signaling promoting recurrence in breast cancer. Kreike *et al.* constructed a gene expression

profile predictive for local recurrence after breast-conserving surgery with postoperative radiotherapy from 343 breast cancer patients.[23] We analyzed the gene expression signature in the breast cancer patients with local recurrence after radiotherapy compared with that of patients without local recurrence by GSEA. The GSEA results showed that breast cancer recurrence after radiotherapy was significantly correlated with upregulation of the TGF-β pathway and EMT (Figure 1A). This data suggest a mechanism by which radiotherapy-induced TGF-β signaling contributed cancer recurrence and metastasis via EMT and cancer cell stemness.

To investigate the anti-metastatic effect of vactosertib, we established a 4T1-Luc allografted BALB/c syngeneic mouse model. GSEA of microarray data of the breast cancer mouse model revealed that TGF-β signaling–related genes were upregulated when the breast cancer model mice were irradiated (Figure 1B). The radiation dose (4 Gy X 3) we set significantly reduced the weight of tumor in mice, and the administered dose of vactosertib (2.5 mg/kg) had no effect on other organs (Figure 1C, Supplementary Figure A). Radiomonotherapy in the 4T1-Luc allografted mouse model considerably increased the metastatic nodules in lung and circulating tumor cell DNA compared with the control group. However, the combination treatment of vactosertib with radiation significantly relieved the risk of lung metastasis compared with radiomonotherapy (Figure 1D). These results suggest that vactosertib combined with radiation may be an effective breast cancer treatment by destroying breast cancer cells and suppressing lung metastasis.

Vactosertib inhibits TGF-ß/Smad signaling

We next examined whether the ALK5 inhibitor vactosertib blocked radiation-induced TGF-β signaling by detecting the phosphorylation of SMAD2/3 both *in vivo* (primary tumors of irradiated 4T1-Luc allografted BALB/c syngeneic mice) and *in vitro* (4T1-Luc cells). p-SMAD2/3 expression in the primary tumor as measured by fluorescence immunohistochemistry (IHC) assay was induced by irradiation and subsequently reduced by co-treatment of vactosertib (Figure 2A). In line with the *in vivo* data, co-treatment of vactosertib significantly reduced the level of p-SMAD2/3 in irradiated 4T1-Luc cells (Figure 2B). Since breast cancer spreads preferentially to the lung[24], we also inves-
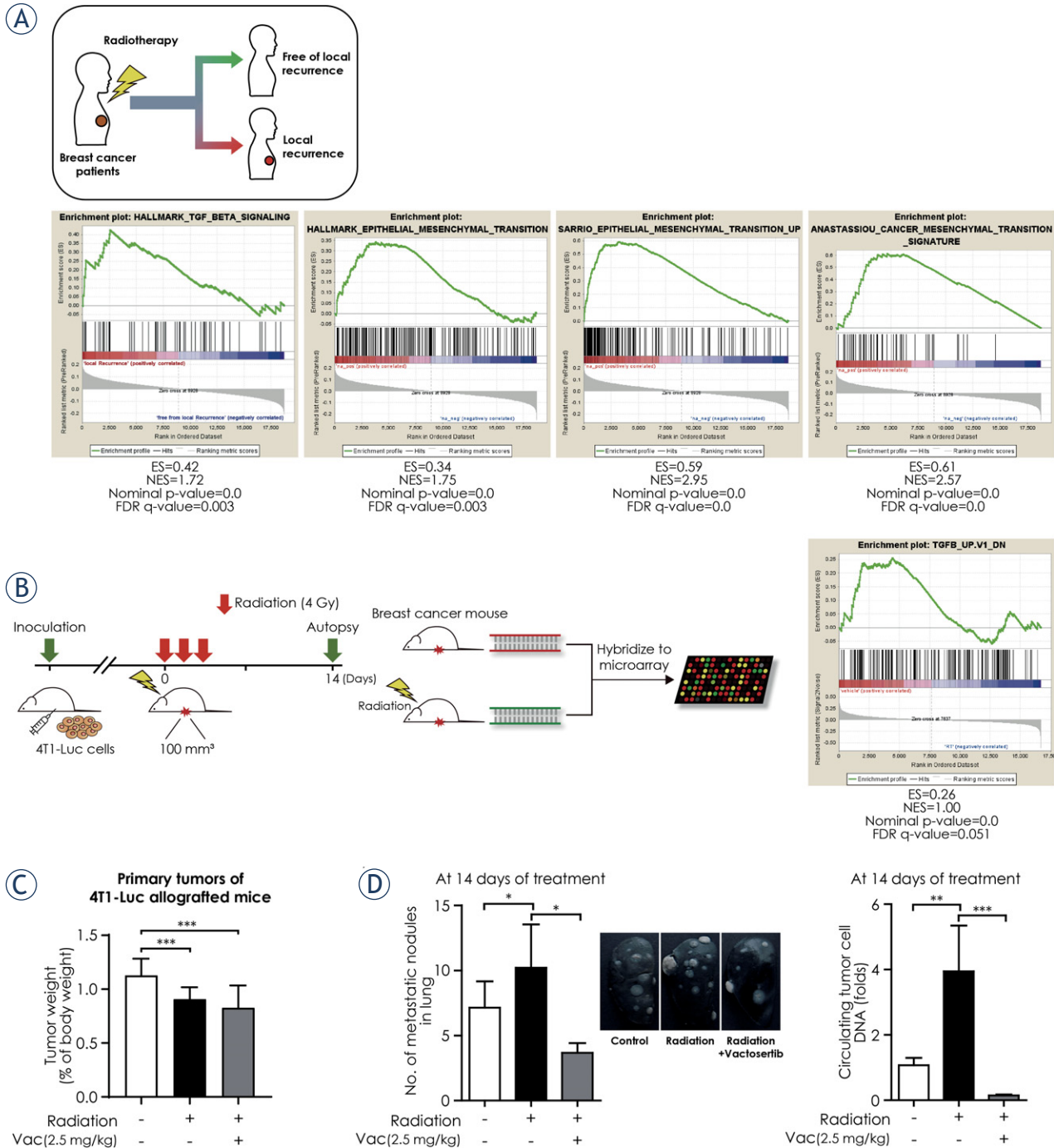
FIGURE 1. Breast cancer recurrence and metastasis after radiotherapy is related to the upregulation of the TGF-β signaling and vactosertib inhibits breast cancer metastasis to the lung. **(A)** Snapshot of gene set enrichment analysis (GSEA) results based on gene-expression profile from the Kreike dataset. The GSEA results showing as enrichment plots suggested that breast cancer recurrence after radiotherapy was significantly correlated with upregulation of the TGF-β pathway and epithelial-to-mesenchymal transition-related gene sets. **(B)** Scheme of the experimental mouse model of breast cancer for radiotherapy (4T1-Luc allografted BALB/c syngeneic mice) and GSEA results based on the gene expression profile from the microarray analysis of the breast cancer mouse model. Mice were injected with 4T1-Luc cells and then divided randomly into two groups (control group and radiotherapy group) when the tumor volume reached 70–100 mm³. The control group received no treatment and the radiotherapy group received whole body irradiation with 4 Gy/day for three days. At 14 days after the first day of radiotherapy, mice were euthanized and breast tumor samples were obtained from each group to perform the microarray analysis. GSEA results based on gene expression profile from the microarray analysis showed that TGF-β signaling–related genes were considerably upregulated in the radiotherapy group. **(C)** Changes in tumor weight in the radiation group and in the radiation and vactosertib combination therapy group compared to the control group. The weight of the tumor in each group was calculated as the relative organ weight to the mouse body weight. **(D)** Vactosertib inhibited breast cancer metastasis to the lung. Inhibition of lung metastasis by vactosertib was evaluated by the number of metastatic nodules in lung using India ink staining.
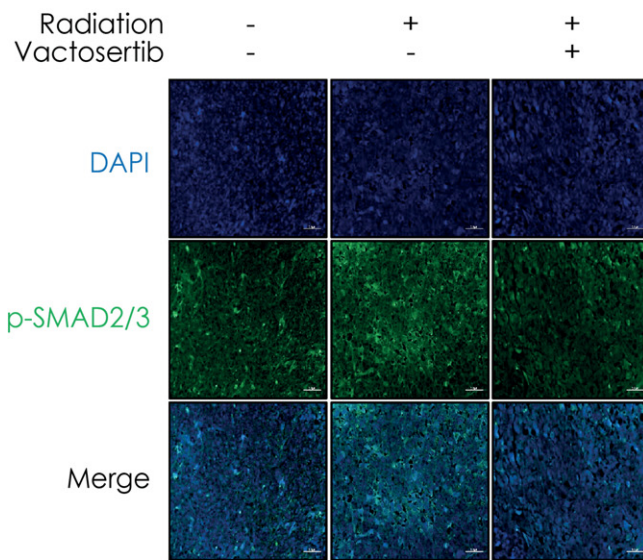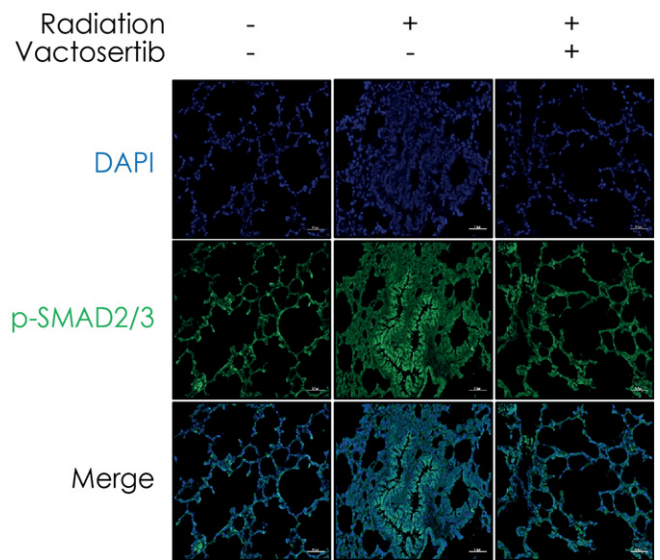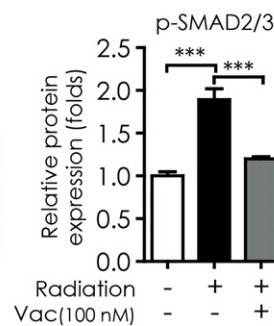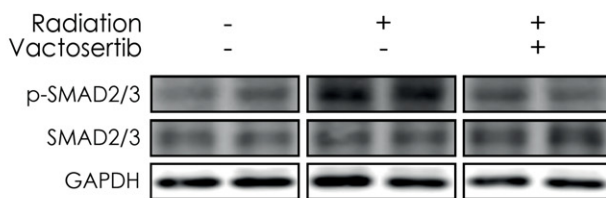
A Primary tumors of 4T1-Luc allografted mice

Lung of 4T1-Luc allografted mice

B 4T1-Luc

FIGURE 2. Vactosertib inhibits TGF-β/Smad signaling. **(A)** Fluorescence immunohistochemistry assay of p-SMAD2/3 in irradiated primary tumors and lung of 4T1-Luc allografted BALB/c syngeneic mice. Protein expression of p-SMAD2/3 was detected by fluorescence immunohistochemistry (magnification: 20×, scale bar: 50 μm). In confocal images, bright green fluorescence indicated p-SMAD2/3. Representative images are shown from three independent experiments. **(B)** Protein expression of p-SMAD2/3 was detected in 4T1-Luc cells by western blot analysis. Protein expression was normalized by that of GAPDH.

tigated the effect of vactosertib in lung tissue of the breast cancer mouse model. The expression of p-SMAD2/3 in lung tissue was elevated after irradiation but co-treatment of vactosertib attenuated this effect. However, the ALK5 inhibitory effect of vactosertib was lower in lung tissue than in the primary tumor (Figure 2A).

Vactosertib attenuates radiation - induced EMT and breast cancer cell migration

Considering that EMT is a significant factor of cancer metastasis, we analyzed EMT markers *in vitro* and *in vivo*. During EMT, upregulation of Smad2/3 induces the expressions of mesenchymal markers, such as the intermediate filament protein *Vimentin* and the extracellular matrix component *Fibronectin*.[4,10] SNAIL acts as a key factor in developing oncogenic EMT and enhancing stem-like properties by suppressing epithelial genes, includ-ing *E-cadherin* and activating mesenchymal genes, including *N-cadherin*.[11] Therefore, we conducted western blot analysis and fluorescence IHC assay to examine whether vactosertib inhibits the induction of VIMENTIN, FIBRONECTIN, SNAIL, and N-CADHERIN by radiation *in vivo*. We found that the protein levels of VIMENTIN, FIBRONECTIN, SNAIL, and N-CADHERIN increased in irradiated primary tumors of 4T1-Luc allografted mice but this increase was significantly abolished by co-treatment of vactosertib (Figure 3A). Consistent with the western blot results, the protein levels of VIMENTIN, FIBRONECTIN, and SNAIL in fluorescence IHC analysis were induced by radiation in primary tumors of 4T1-Luc allografted mice but they were reduced with co-treatment of vactosertib with radiation (Figure 3B).

We also conducted *in vitro* experiments in several breast cancer cell lines to examine the effect of radiation and vactosertib on EMT markers. In 4T1-Luc cells, radiation up-regulated the mRNA expres-
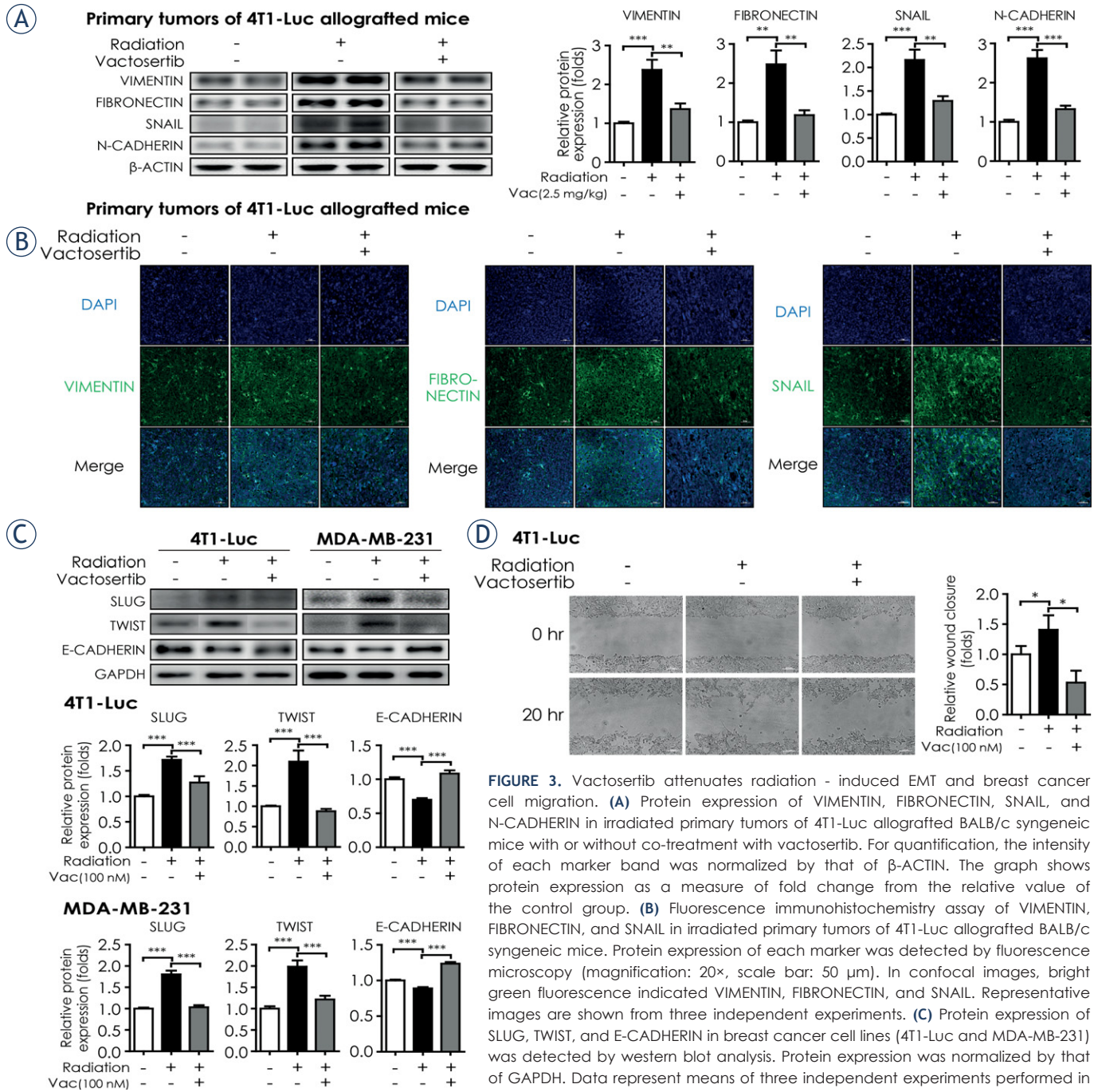
FIGURE 3. Vactosertib attenuates radiation - induced EMT and breast cancer cell migration. **(A)** Protein expression of VIMENTIN, FIBRONECTIN, SNAIL, and N-CADHERIN in irradiated primary tumors of 4T1-Luc allografted BALB/c syngeneic mice with or without co-treatment with vactosertib. For quantification, the intensity of each marker band was normalized by that of β-ACTIN. The graph shows protein expression as a measure of fold change from the relative value of the control group. **(B)** Fluorescence immunohistochemistry assay of VIMENTIN, FIBRONECTIN, and SNAIL in irradiated primary tumors of 4T1-Luc allografted BALB/c syngeneic mice. Protein expression of each marker was detected by fluorescence microscopy (magnification: 20×, scale bar: 50 μm). In confocal images, bright green fluorescence indicated VIMENTIN, FIBRONECTIN, and SNAIL. Representative images are shown from three independent experiments. **(C)** Protein expression of SLUG, TWIST, and E-CADHERIN in breast cancer cell lines (4T1-Luc and MDA-MB-231) was detected by western blot analysis. Protein expression was normalized by that of GAPDH. Data represent means of three independent experiments performed in triplicate. Significance evaluation was performed by one-way analysis of variance (ANOVA) with Bonferroni post-hoc test (*, **, and *** indicate p < 0.05, p < 0.01, and p < 0.005, respectively). **(D)** Effect of vactosertib on the motility of breast cancer cells. The motility of 4T1-Luc cells was measured by wound healing assay. The left panels show the phase contrast microscopic images (magnification: 10×, scale bar: 100 μm) at the start point (0 h) and the end point (20 h). Representative images are shown from three independent experiments. The right graph shows the wound closure as a measure of fold change from the relative value of the control group.

sion of *Vimentin, Fibronectin, Snail,* and *N-cadherin* but co-treatment of vactosertib considerably reduced this effect (Supplementary Figure B1). In line with the result in 4T1-Luc cells, the protein levels of the EMT markers increased in irradiated MDA-MB-231 cells and decreased by co-treatment

of vactosertib (Supplementary Figure B2). In addition to SNAIL, SLUG and TWIST are also EMT-associated transcription factors that repress the expression of *E-cadherin* and stimulate the expression of *N-cadherin*.[11] Therefore, we examined the protein levels of SLUG and TWIST to investigate whether vactosertib blocks the transcriptional activators in developing EMT. *In vitro*, radiation up-regulated the protein levels of SLUG and TWIST but co-treatment of vactosertib reduced their expression both in 4T1-Luc and MDA-MB-231 cells (Figure 3C). Furthermore, we compared the protein level of E-CADHERIN to examine whether vactosertib relieves the radiation-induced mesenchymal traits. In contrast to results with the EMT-associated transcription factors (SLUG, TWIST), the protein level of E-CADHERIN in irradiated 4T1-Luc and MDA-MB-231 cells was decreased compared with that in the control group but it was recovered to a level similar to the control group with co-treatment of vactosertib (Figure 3C).

We next examined the motility of the irradiated breast cancer cells with or without vactosertib treatment by wound healing assay. The wound closure in irradiated 4T1-Luc cells was significantly increased compared with that in non-irradiated 4T1-Luc cells; however, this increase was abolished in irradiated 4T1-Luc cells under the treatment of vactosertib (Figure 3D). These results suggest that radiotherapy promotes metastasis and invasion of cancer cells by inducing mesenchymal traits *in vivo*, and vactosertib may be a promising candidate for an anti-metastatic drug by reducing radiotherapy-induced EMT.

Vactosertib weakens radiation - induced breast cancer stem cell properties.

Radiotherapy can cause metastasis and invasion of cancer cells by promoting EMT and CSC properties, which is mediated by TGF-β signaling.[4] Cancer cells undergoing EMT obtain CSC properties and spread to distant organs.[6,9] Therefore, we investigated whether radiation up-regulates the pluripotent stem cell regulators that play a significant role in the self-renewal of CSCs and whether co-treatment with vactosertib down-regulates these factors. The protein levels of pluripotent stem cell regulators, such as NANOG and Yamanaka's factors (octamer-binding transcription factor 4 (OCT4), sex determining region Y-box 2 (SOX2), Cellular myelocytomatosis oncogene (C-MYC), Kruppel-like factor 4 (KLF4)), were increased in irradiated primary tumor of 4T1-Luc allografted mouse but

decreased by co-treatment with vactosertib as shown by fluorescence IHC analysis (Figure 4A, Supplementary Figure C1). Furthermore, western blot analysis showed that the protein levels of NANOG, OCT4, KLF4, and SCA1 (Stem cell antigen 1) were significantly elevated in irradiated primary tumors of 4T1-Luc allografted mice but co-treatment of vactosertib alleviated these elevations (Figure 4B). Consistent results with *in vivo* data were reproduced in the *in vitro* assays conducted in 4T1-Luc and MDA-MB-231 cells. Radiation induced the mRNA expression of *Nanog* and Yamanaka's factors (*Oct4*, *Sox2*, *c-Myc*, *Klf4*), whereas co-treatment of vactosertib with radiation reduced the mRNA expression of pluripotent stem cell regulators in 4T1-Luc cells (Figure 4C). In addition, the protein levels of the markers increased by radiation and decreased by combinatorial treatment of vactosertib in 4T1-Luc cells and MDA-MB-231 cells as shown by western blot analysis (Figure 4D, Supplementary Figure C2). We also conducted sphere forming assays in breast cancer cell lines to examine whether radiation induces CSC properties such as mammosphere forming ability and if co-treatment of vactosertib abolishes this effect. The results showed that radiation considerably increased mammosphere forming efficiency (MSFE) but vactosertib weakened radiation-induced MSFE in both 4T1-Luc and MDA-MB-231 cells (Figure 4E). Taken together, these results indicate that vactosertib attenuates radiation-induced CSC properties *in vitro* and *in vivo* by repressing the pluripotent stem cell regulators.

Vactosertib suppresses ROS stress generated by radiotherapy.

Radiotherapy damages cancer cells through generating ROS. ROS is also a mediator of radiotherapy-induced EMT with the acquisition of cell stemness via stimulation of transcription factors including SNAIL, Zinc finger E-box-binding homeobox (ZEB), and TWIST that are promoted by various signaling pathways including the TGF-β pathway.[6] Therefore, we conducted *in vitro* experiments and examined several ROS markers to investigate whether vactosertib obstructs oxidative stress generated by radiation. NOX4, one of NADPH oxidases (NOX family members), is activated by the Smad-dependent TGF-β pathway and produces ROS.[25] Western blot confirmed that the protein level of NOX4 was increased in 4T1-Luc and MDA-MB-231 cells after irradiation but it decreased significantly by co-treatment of vactosert-
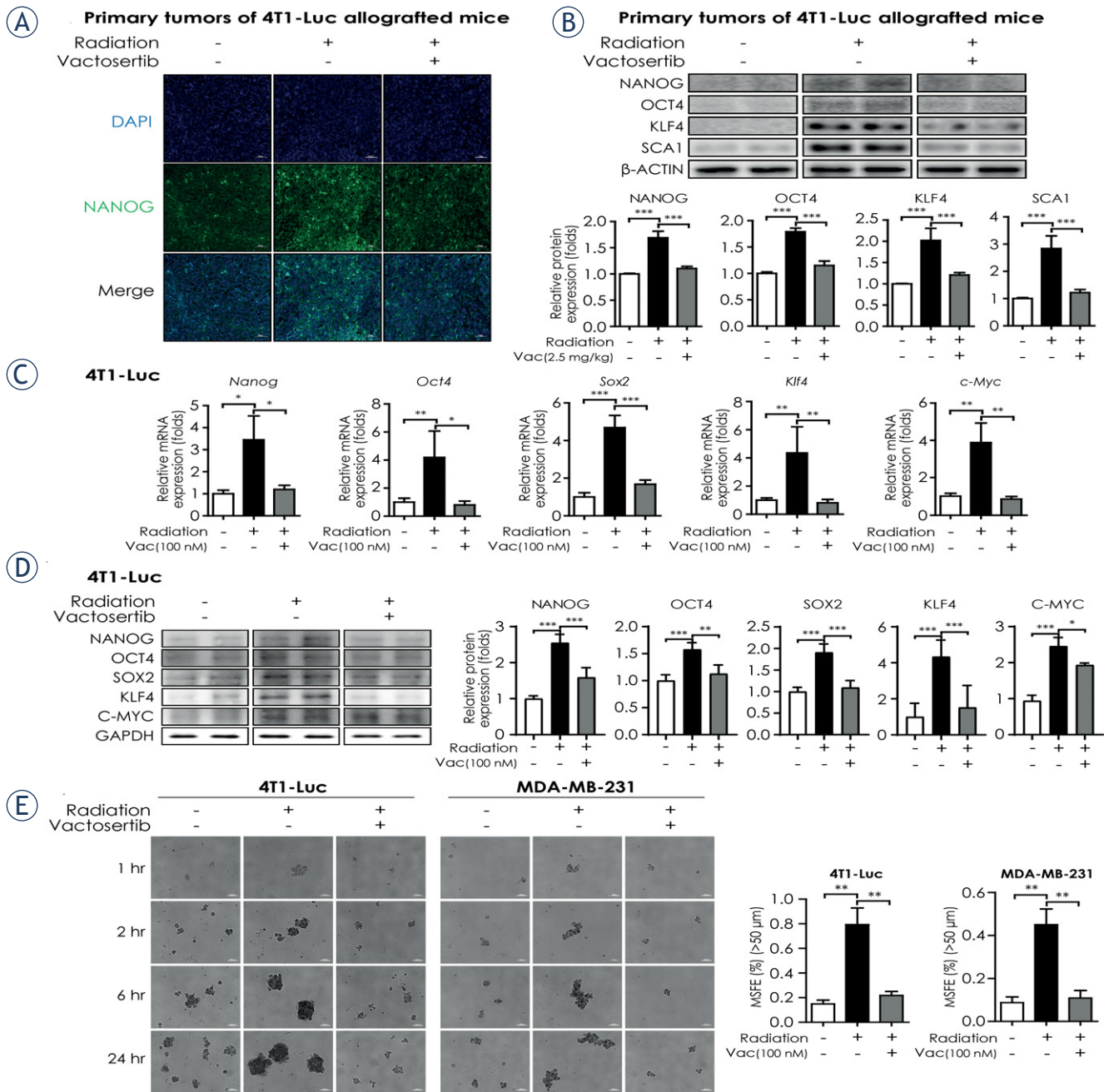
FIGURE 4. Vactosertib weakens radiation – induced breast cancer stem cell properties. **(A)** Fluorescence immunohistochemistry assay of NANOG in irradiated primary tumors of 4T1-Luc allografted BALB/c syngeneic mice. In confocal images, green fluorescence indicates NANOG (magnification: 20×, scale bar: 50 μm). Representative images are shown from three independent experiments. **(B)** Protein expression of cancer stem cell markers (NANOG, OCT4, KLF4, SCA1) in irradiated primary tumors of 4T1-Luc allografted BALB/c syngeneic mice with or without co-treatment with vactosertib. For quantification, protein expression was normalized by that of β-ACTIN. The graph shows the protein expression of each marker as a measure of fold change from the relative value of the control group. **(C)** Relative mRNA expression of pluripotent stem cell regulators (Nanog, Oct4, Sox2, c-Myc and Klf4) in 4T1-Luc cells. The mRNA expression level was normalized by that of Ppia mRNA. **(D)** Protein expression of pluripotent stem cell regulators (NANOG, OCT4, SOX2, C-MYC and KLF4) in 4T1-Luc cells was determined by western blot analysis. Protein expression was normalized by that of GAPDH. Data represent means of three independent experiments performed in triplicate. Significance evaluation was performed by one-way analysis of variance (ANOVA) with Bonferroni post-hoc test (*, **, and *** indicate p < 0.05, p < 0.01, and p < 0.005, respectively). **(E)** Radiation-induced mammosphere formation ability in breast cancer cell lines (4T1-Luc and MDA-MB-231). Breast cancer cells were irradiated with 10 Gy with or without 30-min pretreatment with vactosertib (100 nM). After 1, 2, 6, and 24 h of incubation, cells were reseeded in ultra-low attachment dishes and cultured for seven days. The left panels show the phase contrast microscopic images of spheres after seven days of culture in the ultra-low attachment condition (magnification: 5x, scale bar: 200 μm). Representative images are shown from three independent experiments. The right graph shows the mammosphere forming efficiency (MSFE) based on the number of spheres (> 50 μm) from 24 h–incubated cells.
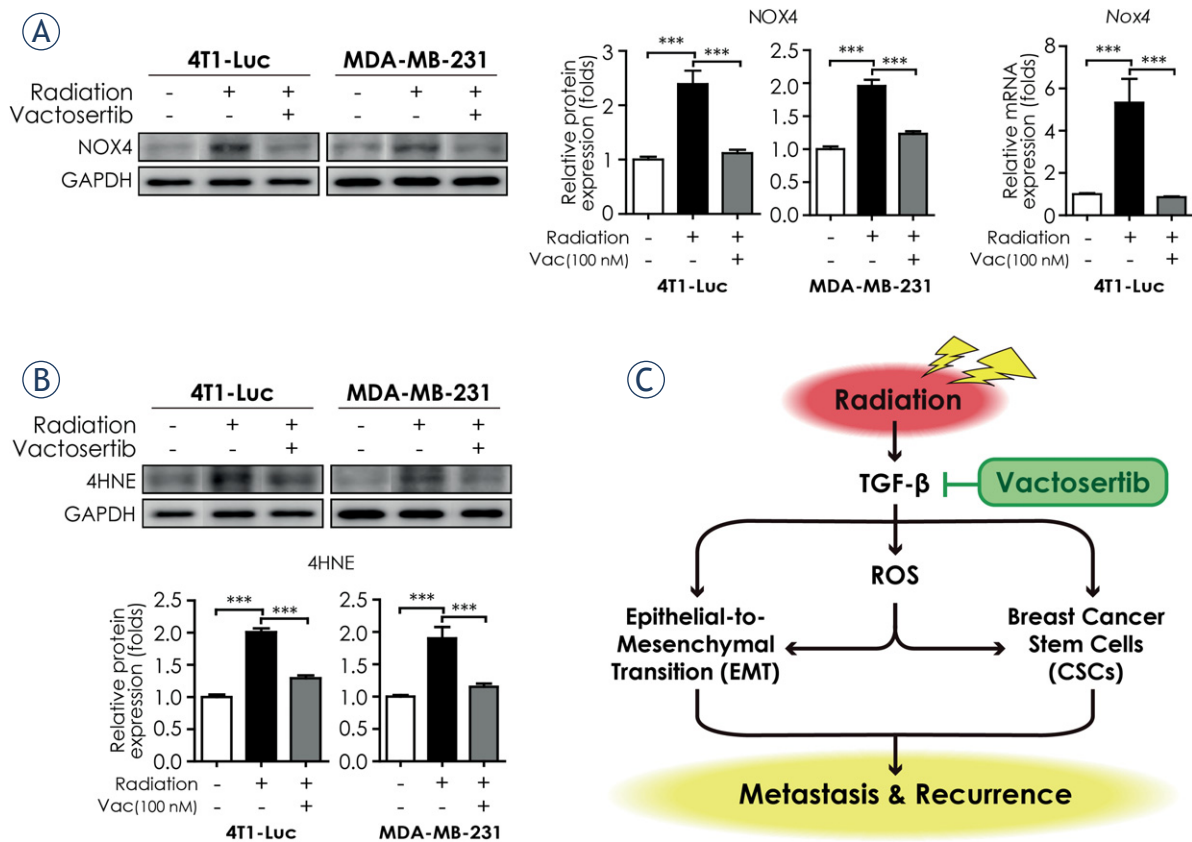
FIGURE 5. Vactosertib suppresses ROS stress generated by radiotherapy. **(A)** Protein and mRNA expression of NOX4 in breast cancer cell lines (4T1-Luc and MDA-MB-231). Protein expression of NOX4 in 4T1-Luc and MDA-MB-231 cells were analyzed by western blot analysis. Protein expression was normalized by that of GAPDH. The mRNA expression level of Nox4 in 4T1-Luc cells was analyzed by quantitative reverse transcription¬–polymerase chain reaction. The mRNA expression level of Nox4 was normalized by that of Ppia mRNA. **(B)** Protein expression of 4HNE in 4T1-Luc and MDA-MB-231 cells was determined by western blot analysis. Protein expression was normalized by that of GAPDH. Data represent means of three independent experiments performed in triplicate. Significance evaluation was performed by one-way analysis of variance (ANOVA) with Bonferroni post-hoc test (*, **, and *** indicate $p < 0.05$, $p < 0.01$, and $p < 0.005$, respectively). **(C)** Summary plot of radiation-induced epithelial-to-mesenchymal transition (EMT), breast cancer stem cells, and ROS stress generation mediated by TGF-β signaling. TGF-β-induced EMT and CSC properties promote metastasis to distant organs and cancer recurrence. An ALK5 inhibitor, vactosertib, suppresses TGF-β-induced EMT, CSC properties, and ROS stress generation. Vactosertib may be an attractive strategy for prevention of cancer metastasis and recurrence in breast cancer patients undergoing radiotherapy.

ib. The mRNA expression of *Nox4* also showed a similar pattern in irradiated 4T1-Luc cells in qRT-PCR analysis (Figure 5A). Another biomarker of oxidative stress, 4-hydroxy-2,3-nonenal (4-HNE), is a product of lipid peroxidation.[19] 4-HNE is one of the most powerful reactive aldehydes and stimulates the TGF-β pathway.[26] We observed that the elevated protein level of 4-HNE in irradiated breast cancer cell lines decreased by concomitant treatment with vactosertib in western blot analysis (Figure 5B). These data suggest that vactosertib may mitigate radiotherapy-induced EMT and cancer cell stemness by inhibiting ROS stress, which is also generated by radiotherapy.

Discussion

Even though radiotherapy is one of the necessary adjuvant treatment modalities for the management of breast cancer, some patients fail to benefit from radiotherapy as evidenced by cancer metastasis and recurrence.[27] A number of studies have shown that the development of EMT and CSCs following radiotherapy promotes the ability of breast cancer cells to acquire metastatic properties.[1,28-30] This mechanism was recognized as a limitation of single radiation therapy[31], and the need for a new treatment strategy to prevent metastasis and recurrence was emphasized. Small molecules inhib-

iting TGF-β/ALK5 kinase, vactosertib effectively inhibited lung metastasis from breast cancer in a mouse model and has been investigated in various ongoing clinical trials with cancer patients.[16,18,32] For example, galunisertib (LY2157299) combined with radiotherapy is currently being investigated in a phase I clinical trial with advanced hepatocellular cancer patients to evaluate the safety and efficacy outcomes including the effect of inhibiting TGF-β signaling (NCT02906397). Previous studies showed that vactosertib inhibited TGF-β-induced ROS stress, morphological change, cell invasion and metastasis of breast cancer cells more strongly than galunisertib *in vitro* and *in vivo*.[18,19] In addition, a clinical study (NCT03724851) to evaluate the efficacy and safety of vactosertib and pembrolizumab combination treatment in patients with metastatic colorectal cancer (mCRC) is in progress.[32] In the MP-VAC-204 study, vactosertib in combination with pembrolizumab demonstrated antitumor efficacy by immunorecovery and inhibition of TGF-β signaling in previously chemotherapy-treated mCRC patients.[33] Therefore, we found that radiation-induced TGF-β pathway correlates with EMT by analyzing gene expression characteristics of patients with breast cancer who received local recurrence after radiotherapy.[23] These findings suggest the possibility that inhibition of TGF-β signaling can prevent radiation-induced cancer metastasis and recurrence.

Understanding the molecular mechanism of the radiation-induced TGF-β pathway is important for finding effective treatment options. Interestingly, we identified lung metastases in a mouse model that received mono-radiotherapy and showed that they were attenuated by combination treatment with Vactosertib (Figure 1C). In addition, the combination of radiation and Vactosertib downregulated p-Smad2/3 in mouse cancer and lung (Figure 2), indicating that it could be a predictive marker for lung metastasis.[21,34] Previous studies demonstrated that vactosertib reduced metastatic properties of human lung cancer cells via inhibition of EMT enhanced by TGF-β.[34] Furthermore, Park et al. previously reported that vactosertib suppressed paclitaxel-induced EMT and CSC properties by inhibiting SNAIL through TGF-β signaling.[9] Considering that high expression of SNAIL in breast cancer implies aggressive progression and poor prognosis as evidenced by cancer metastasis and recurrence, the inhibitory effect of vactosertib on SNAIL and mesenchymal traits generated by radiation deserves attention as a therapeutic strategy to enhance the efficacy of radiotherapy in breast

cancer patients.[35] Here we focused on whether any markers associated with EMT and CSC respond by TGF-β signaling. The radiation-induced TGF-β signaling cascade resulted in activation of EMT inducers such as Snail, Twist, and Slug and upregulation of mesenchymal markers such as N-cadherin, vimentin, and Fibronectin (Figure 3). Some researchers have described that cancer cells acquire invasive and metastatic phenotypes during EMT and induce the expression of mesenchymal markers by suppressing the expression of epithelial markers such as E-cadherin.[34,36] Although numerous studies have reported that cancer cells undergoing radiotherapy-induced EMT gain CSC properties, the underlying signaling pathways are still unknown and could be induced by TGF-β and other proteins.[6,37] we demonstrated the acquisition of cancer stem cell characteristics by radiation by confirming the expression of NANOG and Yamanaka's factors (OCT4, SOX2, C-MYC, KLF4) and the formation of mammospheres for cells. Vactosertib not only inhibited highly expressed EMT and CSC, but also showed downregulation of ROS markers such as NOX4 and 4-HNE. In a previous study, vactosertib showed anti-fibrotic effects by inhibition of both canonical and non-canonical ROS signaling of the TGF-β pathway in fibrotic disease models.[19] As mentioned earlier, changes in the tumor microenvironment caused by irradiation can induce a cancer stem cell phenotype and are related to ROS-induced oxidative stress.[3,38] ROS is produced by mitochondrial damage and has been shown to play an important role in EMT.[39] Several studies have demonstrated that radiation may increase the level of ROS and induce tumor progression by ROS, which may increase metastasis.[38,40,41]

In conclusion, we have demonstrated that cotreatment of the orally bioavailable vactosertib with radiotherapy may improve the outcome of breast cancer treatment by suppressing EMT, cancer cell stemness, ROS stress generation, and metastasis to other organs. We therefore propose that this combination therapy has a great potential for clinical application for breast cancer patients.

Reference

1. Ko YS, Jin H, Lee JS, Park SW, Chang KC, Kang KM, et al. Radioresistant breast cancer cells exhibit increased resistance to chemotherapy and enhanced invasive properties due to cancer stem cells. *Oncol Rep* 2018; **40**: 3752-62. doi: 10.3892/or.2018.6714

2. Begg AC, Stewart FA, Vens C. Strategies to improve radiotherapy with targeted drugs. *Nat Rev Cancer* 2011; **11**: 239-53. doi: 10.1038/nrc3007

3. Barker HE, Paget JT, Khan AA, Harrington KJ. The tumour microenvironment after radiotherapy: mechanisms of resistance and recurrence. *Nat Rev Cancer* 2015; **15**: 409-25. doi: 10.1038/nrc3958

4. Farhood B, Khodamoradi E, Hoseini-Ghafarokhi M, Motevaseli E, Mirtavoos-Mahyari H, Eleojo Musa A, et al. TGF-β in radiotherapy: Mechanisms of tumor resistance and normal tissues injury. *Pharmacol Res* 2020; **155:** 104745. doi: 10.1016/j.phrs.2020.104745

5. Torre LA, Bray F, Siegel RL, Ferlay J, Lortet-Tieulent J, Jemal A. Global cancer statistics, 2012. *CA Cancer J Clin* 2015; **65:** 87-108. doi: 10.3322/caac.21262

6. Lee SY, Jeong EK, Ju MK, Jeon HM, Kim MY, Kim CH, et al. Induction of metastasis, cancer stem cell phenotype, and oncogenic metabolism in cancer cells by ionizing radiation. *Mol Cancer* 2017; **16:** 10. doi: 10.1186/s12943-016-0577-4

7. Dancea HC, Shareef MM, Ahmed MM. Role of radiation-induced TGF-beta signaling in cancer therapy. *Mol Cell Pharmacol* 2009; **1:** 44-56. doi: 10.4255/mcpharmacol.09.06

8. Hong E, Park S, Ooshima A, Hong CP, Park J, Heo JS, et al. Inhibition of TGF-β signalling in combination with nal-IRI plus 5-Fluorouracil/Leucovorin suppresses invasion and prolongs survival in pancreatic tumour mouse models. *Sci Rep* 2020; **10:** 2935. doi: 10.1038/s41598-020-59893-5

9. Park SY, Kim MJ, Park SA, Kim JS, Min KN, Kim DK, et al. Combinatorial TGF-β attenuation with paclitaxel inhibits the epithelial-to-mesenchymal transition and breast cancer stem-like cells. *Oncotarget* 2015; **6:** 37526-43. doi: 10.18632/oncotarget.6063

10. Singh A, Settleman J. EMT, cancer stem cells and drug resistance: an emerging axis of evil in the war on cancer. *Oncogene* 2010; **29:** 4741-51. doi: 10.1038/onc.2010.215

11. Diepenbruck M, Christofori G. Epithelial-mesenchymal transition (EMT) and metastasis: yes, no, maybe? *Curr Opin Cell Biol* 2016; **43:** 7-13. doi: 10.1016/j.ceb.2016.06.002

12. Pastushenko I, Blanpain C. EMT transition states during tumor progression and metastasis. *Trends Cell Biol* 2019; **29:** 212-26. doi: 10.1016/j.tcb.2018.12.001

13. Wang Y, Yu Y, Tsuyada A, Ren X, Wu X, Stubblefield K, et al. Transforming growth factor-β regulates the sphere-initiating stem cell-like feature in breast cancer through miRNA-181 and ATM. *Oncogene* 2011; **30:** 1470-80. doi: 10.1038/onc.2010.531

14. Fuxe J, Vincent T, Garcia de Herreros A. Transcriptional crosstalk between TGF-β and stem cell pathways in tumor cell invasion: role of EMT promoting Smad complexes. *Cell Cycle* 2010; **9:** 2363-74. doi: 10.4161/cc.9.12.12050

15. Keedy VL, Bauer TM, Clarke JM, Hurwitz H, Baek I, Ha I, et al. Association of TGF-β responsive signature with anti-tumor effect of vactosertib, a potent, oral TGF-β receptor type I (TGFBRI) inhibitor in patients with advanced solid tumors. [abstract]. *J Clin Oncol* 2018; **36(15 Suppl):** 3031. doi: 10.1200/JCO.2018.36.15_SUPPL.3031

16. Jung SY, Hwang S, Clarke JM, Bauer TM, Keedy VL, Lee H, et al. Pharmacokinetic characteristics of vactosertib, a new activin receptor-like kinase 5 inhibitor, in patients with advanced solid tumors in a first-in-human phase 1 study. *Invest New Drugs* 2020; **38:** 812-20. doi: 10.1007/s10637-019-00835-y

17. Jin CH, Krishnaiah M, Sreenu D, Subrahmanyam VB, Rao KS, Lee HJ, et al. Discovery of N-((4-([1,2,4]triazolo[1,5-a]pyridin-6-yl)-5-(6-methylpyridin-2-yl)-1H-imidazol-2-yl)methyl)-2-fluoroaniline (EW-7197): a highly potent, selective, and orally bioavailable inhibitor of TGF-β type I receptor kinase as cancer immunotherapeutic/antifibrotic agent. *J Med Chem* 2014; **57:** 4213-38. doi: 10.1021/jm500115w

18. Son JY, Park SY, Kim SJ, Lee SJ, Park SA, Kim MJ, et al. EW-7197, a novel ALK-5 kinase inhibitor, potently inhibits breast to lung metastasis. *Mol Cancer Ther* 2014; **13:** 1704-16. doi: 10.1158/1535-7163.MCT-13-0903

19. Park SA, Kim MJ, Park SY, Kim JS, Lee SJ, Woo HA, et al. EW-7197 inhibits hepatic, renal, and pulmonary fibrosis by blocking TGF-β/Smad and ROS signaling. *Cell Mol Life Sci* 2015; **72:** 2023-39. doi: 10.1007/s00018-014-1798-6

20. Yoon JH, Jung SM, Park SH, Kato M, Yamashita T, Lee IK, et al. Activin receptor-like kinase5 inhibition suppresses mouse melanoma by ubiquitin degradation of Smad4, thereby derepressing eomesodermin in cytotoxic T lymphocytes. *EMBO Mol Med* 2013; **5:** 1720-39. doi: 10.1002/emmm.201302524

21. Park S, Yang KM, Park Y, Hong E, Hong CP, Park J, et al. Identification of epithelial-mesenchymal transition-related target genes induced by the mutation of Smad3 linker phosphorylation. *J Cancer Prev* 2018; **23:** 1-9. doi: 10.15430/JCP.2018.23.1.1

22. Jung SY, Yug JS, Clarke JM, Bauer TM, Keedy VL, Hwang S, et al. Population pharmacokinetics of vactosertib, a new TGF-β receptor type I inhibitor, in patients with advanced solid tumors. *Cancer Chemother Pharmacol* 2020; **85:** 173-83. doi: 10.1007/s00280-019-03979-z

23. Servant N, Bollet MA, Halfwerk H, Bleakley K, Kreike B, Jacob L, et al. Search for a gene expression signature of breast cancer local recurrence in young women. *Clin Cancer Res* 2012; **18:** 1704-15. doi: 10.1158/1078-0432.CCR-11-1954

24. Jin L, Han B, Siegel E, Cui Y, Giuliano A, Cui X. Breast cancer lung metastasis: Molecular biology and therapeutic implications. *Cancer Biol Ther* 2018; **19:** 858-68. doi: 10.1080/15384047.2018.1456599

25. Samarakoon R, Overstreet JM, Higgins PJ. TGF-β signaling in tissue fibrosis: redox controls, target genes and therapeutic opportunities. *Cell Signal* 2013; **25:** 264-8. doi: 10.1016/j.cellsig.2012.10.003

26. Breitzig M, Bhimineni C, Lockey R, Kolliputi N. 4-Hydroxy-2-nonenal: a critical target in oxidative stress? *Am J Physiol Cell Physiol* 2016; **311:** C537-C543. doi: 10.1152/ajpcell.00101.2016

27. Langlands FE, Horgan K, Dodwell DD, Smith L. Breast cancer subtypes: response to radiotherapy and potential radiosensitisation. *Br J Radiol* 2013; **86:** 20120601. doi: 10.1259/bjr.20120601

28. Tripathy J, Chowdhury AR, Prusty M, Muduli K, Priyadarshini N, Reddy KS, et al. α-Lipoic acid prevents the ionizing radiation-induced epithelial-mesenchymal transition and enhances the radiosensitivity in breast cancer cells. *Eur J Pharmacol* 2020; **871:** 172938. doi: 10.1016/j.ejphar.2020.172938

29. Hou J, Li L, Zhu H, Chen H, Wei N, Dai M, et al. Association between breast cancer cell migration and radiosensitivity *in vitro*. *Oncol Lett* 2019; **18:** 6877-84. doi: 10.3892/ol.2019.11027

30. Lagadec C, Vlashi E, Della Donna L, Dekmezian C, Pajonk F. Radiation-induced reprogramming of breast cancer cells. *Stem Cells* 2012; **30:** 833-44. doi: 10.1002/stem.1058

31. Sundahl N, Duprez F, Ost P, De Neve W, Mareel M. Effects of radiation on the metastatic process. *Mol Med* 2018; **24:** 16. doi: 10.1186/s10020-018-0015-8

32. Kim BG, Malek E, Choi SH, Ignatz-Hoover JJ, Driscoll JJ. Novel therapies emerging in oncology to target the TGF-β pathway. *J Hematol Oncol* 2021; **14:** 55. doi: 10.1186/s13045-021-01053-x

33. Kim TW, Lee KW, Ahn JB, Park YS, Ock CY, Park H, et al. Tumor microenvironment based on PD-L1 and CD8 T-cell infiltration correlated with the response of MSS mCRC patients treated vactosertib in combination with pembrolizumab. [abstract]. *J Immunother Cancer 2021;* **9(Suppl 2):** A82. Abstr. No. 74. doi: 10.1136/jitc-2021-SITC2021.074

34. Kaowinn S, Kim J, Lee J, Shin DH, Kang CD, Kim DK, et al. Cancer upregulated gene 2 induces epithelial-mesenchymal transition of human lung cancer cells via TGF-β signaling. *Oncotarget* 2017; **8:** 5092-110. doi: 10.18632/oncotarget.13867

35. Chang HY, Tseng YK, Chen YC, Shu CW, Lin MI, Liou HH, et al. High snail expression predicts a poor prognosis in breast invasive ductal carcinoma patients with HER2/EGFR-positive subtypes. *Surg Oncol* 2018; **27:** 314-20. doi: 10.1016/j.suronc.2018.05.002

36. Wang Y, Shi J, Chai K, Ying X, Zhou BP. The role of Snail in EMT and tumorigenesis. *Curr Cancer Drug Targets* 2013; **13:** 963-72. doi: 10.2174/15680096113136660102

37. Yadav P, Shankar BS. Radio resistance in breast cancer cells is mediated through TGF-β signalling, hybrid epithelial-mesenchymal phenotype and cancer stem cells. *Biomed Pharmacother* 2019; **111:** 119-30. doi: 10.1016/j.biopha.2018.12.055

38. Wang Y, Shi J, Chai K, Ying X, Zhou BP. Induction of metastasis, cancer stem cell phenotype, and oncogenic metabolism in cancer cells by ionizing radiation. *Mol Cancer* 2017; **16:** 10. doi: 10.1186/s12943-016-0577-4

39. Sim JJ, Jeong KY. Monitoring epithelial-mesenchymal transition of pancreatic cancer cells via investigation of mitochondrial dysfunction. *Methods Protoc* 2020; **3:** 32. doi: 10.3390/mps3020032

40. Karicheva O, Rodriguez-Vargas JM, Wadier N, Martin-Hernandez K, Vauchelles R, Magroun N, et al. PARP3 controls TGFβ and ROS driven epithelial-to-mesenchymal transition and stemness by stimulating a TG2-Snail-E-cadherin axis. *Oncotarget* 2016; **7:** 64109-23. doi: 10.18632/oncotarget.11627

41. Sonowal H, Ramana KV. 4-Hydroxy-Trans-2-Nonenal in the regulation of anti-oxidative and pro-inflammatory signaling pathways. *Oxid Med Cell Longev* 2019; **2019:** 5937326. doi: 10.1155/2019/5937326